RSC Advances

PAPER

View Article Online
View Journal | View Issue

Cite this: *RSC Adv.*, 2023, **13**, 3541

Self-lubrication and tribological properties of polymer composites containing lubricant

Sung-Jun Lee,[a] Gang-Min Kim[b] and Chang-Lae Kim *[a]

Received 27th December 2022
Accepted 17th January 2023

DOI: 10.1039/d2ra08262d

rsc.li/rsc-advances

The purpose of this study was to improve the tribological properties of polydimethylsiloxane (PDMS) by mixing lubricants into it. The chemical composition, physical/chemical bonding state, and mechanical properties of the PDMS/lubricant composites (PLCs), prepared by mixing PDMS and lubricants at different ratios, were analyzed. With increasing lubricant content, the friction coefficient initially decreased, reaching a minimum value at a PDMS/lubricant ratio of 100 : 10; however, it gradually increased with a further increase in the lubricant content. The mechanical properties of PLCs with lubricant contents of 10% and higher decreased owing to the lubricant addition, so that the contact area with the sliding counter tip increased with lubricant content, but the frictional resistance was still decreased owing to the self-lubricating effect. In addition, owing to the effect of the lubricating film, there was no direct contact between the PLC surface and counter tip, and almost no damage was done to the PLC surface. Finite element analysis of the changes in stress during indentation and sliding confirmed that the stress applied to the PLCs was lower than that for bare PDMS.

1 Introduction

Polydimethylsiloxane (PDMS) is a viscoelastic material produced by mixing the main and curing agents at a certain ratio and curing the mixture by applying heat.[1–3] PDMS exhibits excellent flexibility, moldability, and other mechanical properties, and the bonding strength between polymer chains in it depends on the content of the curing agent.[4–6] However, viscoelastic materials form an adhesive bond with the counterpart material through van der Waals forces;[7,8] furthermore, the elasticity of the material leads to greater contact area, so after the elastic material is adhered to another surface, a compressive force and restoring force are generated owing to its elasticity, and a large amount of energy is required to overcome the adhesive force.[9,10] This causes viscoelastic/adhesive materials to exhibit high frictional forces.

Lubricants are typically used to decrease the adhesive force of viscoelastic materials.[11–13] Lubrication reduces the area of direct contact between the two surfaces by forming a lubricating film between them and replaces friction between the material surfaces with friction between the counter material and the lubricating film. As a result, the lubricating film reduces the frictional force, thereby reducing the wear damage to the material surface.[14,15] However, general lubricants are problematic to use with PDMS in electronics and biomedical field.[16,17] Even if a suitable lubricant is applied on the PDMS surface, the lubricant is lost over time and must be periodically injected.

Recently, the friction and wear properties of PDMS have been improved through the addition of nano/micro-sized particles during mixing of the PDMS base and curing agent.[18,19] However, although nano/micro particles initially reduced friction, they gnawed the relatively weak PDMS surface. Accordingly, permanent patterning on the PDMS surface, without the addition of other particles, has also been reported.[20–22] However, in these studies, a mold for patterning the PDMS surface had to be manufactured separately. In addition, the friction force considerably increased when the counter tip sliding on the PDMS surface caught on the patterns; furthermore, the patterns were eventually damaged by repeated contact sliding for a long time. Although studies have been conducted to improve the friction and wear characteristics of PDMS in various ways, multiple problems remain.

In this study, a PDMS/lubricant composite (PLC) with self-lubricating properties and abrasion resistance was prepared by adding a lubricant to PDMS. To determine the optimal mixing ratio, changes in chemical composition and chemical bonding at multiple PDMS/lubricant ratios were analyzed, and the corresponding surface, mechanical, and tribological properties were evaluated under various conditions.

2 Materials and methods

2.1 Materials and methods

The lubricant (Super Lube, New York, USA) used in this study is composed of an unspecified ratio of polytetrafluoroethylene

[a]*Department of Mechanical Engineering, Chosun University, Gwangju, 61452, Republic of Korea. E-mail: kimcl@chosun.ac.kr*

[b]*Korea Automotive Technology Institute, Yeongam-gun, 58463, Republic of Korea*

(PTFE) (<5%) in a polyalphaolefin (PAO) (<85%) fluid, and its main components are PTFE and PAO. This lubricant is mainly used to prevent damage caused by contact, vibration, and extreme environments.[23,24] PTFE is a non-adhesive and low-friction material that is primarily used for the fabrication of hydrophobic/non-adhesive surfaces.[25] Owing to the non-adhesive properties of PTFE, its friction coefficient is usually low, but PTFE easily wears out.[26] PAO is used in lubricants in various fields, for instance in automobile engine oil and transmission oil.[27]

The addition of PTFE and PAO to PDMS (SYLGARD 184, Dow, Seoul, Korea) is expected to improve its friction properties owing to the excellent lubricity of PAO and low friction properties of PTFE. However, if the mixing ratio of PDMS to lubricant is inappropriate, the resulting PLC may have poor mechanical properties and low wear resistance.[28] PLC specimens with PDMS/lubricant ratios of $100:x$ ($x = 1$, 5, 10, 20, and 30) were prepared. As shown in Fig. 1, PDMS (PDMS base and curing agent mixed at a ratio of 10 : 1), was poured into a Petri dish, and the lubricant was added according to the mixing ratio. After curing at room temperature for 24 h, the cured specimen of approximately 2 mm in thickness was cut to a size of 15 mm × 15 mm for subsequent use in the experiment. As shown in Table 1, in this study, the 100% PDMS specimen without lubricant is denoted as bare PDMS, and samples of PDMS with lubricant added at PMDS/lubricant ratios of $100:x$ are called PLC-x, where $x = 1$, 5, 10, 20, and 30.

2.2 Experiments

Quantitative and qualitative chemical composition analyses of PLCs were performed using attenuated total reflectance Fourier transform infrared spectroscopy (FTIR; Nicolet 6700, Thermo Scientific, Seoul, Korea). In a state where PDMS and the lubricant were mixed, absorbance analysis of each specimen according to the mixing ratio was performed by measuring the wavenumbers in the range of 500–4000 cm^{-1}

The droplet contact angles on the surfaces of the PLCs and their surface roughness were measured. After dropping 10 μL of deionized water onto the surface of the specimen, and the contact angle of the water droplet on the surface was measured using a microscope camera (U1000X, Wtong Industry Group, Seoul, Korea). The surface roughness of the specimens was measured using 3D laser scanning confocal microscopy (3D LSCM, VK-X200, KEYENCE, Osaka, Japan).

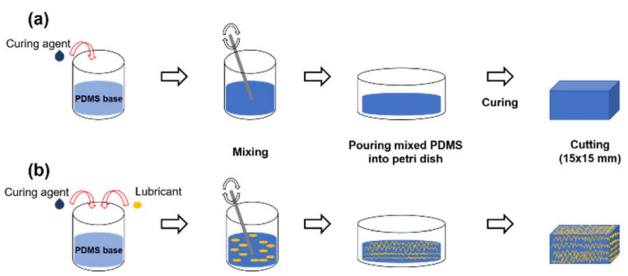

Fig. 1 Fabrication process of (a) bare PDMS, and (b) PLCs.

An indentation test was performed to evaluate the mechanical properties of the PLCs with different lubricant contents. The indenter was put in contact with the surface of the specimen; then, it was pressed down and returned to its original position, and the force was determined based on the indentation depth. The experimental conditions are listed in Table 2. The indenter (a steel ball with a size of 25.4 mm) was loaded at a constant speed of 0.3 mm s^{-1}, pressed into the surface of the specimen, and unloaded at the same speed. The maximum load applied to the specimen surface was 1 N. In this process, the change in the load was determined based on the indentation depth.

A tribotester (RFW 160, NEOPLUS, Co., Ltd, Daejeon, Korea) with a reciprocating sliding motion was used to evaluate the friction and wear characteristics of the specimens. The reciprocating sliding-type tribotester had a driving mechanism that converts the rotational motion of the cam connected to the motor into a linear motion to enable repeated sliding motion. The tribotest conditions are presented in Table 3. The counter tip was a steel ball with a mechanical strength higher than that of PDMS, and the diameter of the steel ball was 1 mm. After the specimen was fixed on the stage that reciprocated with a stroke of 2 mm, a normal load was applied while the counter tip was in contact with the specimen surface, and then sliding movement was performed. The normal loads were 100, 300, and 500 mN, the sliding speeds were 4 and 16 mm s^{-1}, and the numbers of sliding cycles were 10 000, 100 000, and 500 000. All other experimental conditions were the same, and each experiment was repeated three or more times to ensure the reliability of the experimental results. At the end of the experiment, the wear morphology of the specimen surface was analyzed using 3D LSCM, and the width, depth, and volume of the wear tracks were evaluated.

3 Results and discussion

Fig. 2 shows the FTIR spectra of the PLCs. The peaks at 2856 and 2960 cm^{-1} were ascribed to the symmetric/asymmetric expansion and contraction of methylene, indicating the properties of hydrocarbons.[29] The peak at 1413 cm^{-1} was attributed to the deformation/dissymmetry deformation vibrations of methyl groups linked to silicon atoms.[30] The peaks at 755 and 1168 cm^{-1} peaks were ascribed to the bending vibration of C–H, and peaks at 1750 and 1160 cm^{-1} are the absorption bands of the carbonyl group.[31] The peak at 1260 cm^{-1} corresponds to CF_3 and those at 1091 and 688 cm^{-1} correspond to CF_2, which are considered responsible for the hydrophobicity of PTFE.[32] The absorption peaks at 1062, 1012, and 790 cm^{-1}, ascribed to Si–O–Si stretching vibrations, are the main absorption peaks of PDMS.[33] The peak at 1590 cm^{-1} were attributed to C–O bonds formed by the PDMS base and curing agent, and the peaks at 1062 and 1259 cm^{-1} were ascribed to symmetric/asymmetric stretching of the C–F bond.[34,35] The main peaks of bare PDMS and PLCs are similar due to the presence of CH and Si components, but the peaks at 1260, 1091, and 688 cm^{-1} are characteristic of PTFE and indicate differences in absorption bands. With increasing lubricant content, the intensity of the

Table 1 Specimen names according to the mixing ratio of PDMS : lubricant

Mixing ratio (PDMS : lubricant)	100 : 0	100 : 1	100 : 5	100 : 10	100 : 20	100 : 30
Specimen designation	Bare PDMS	PLC-1	PLC-5	PLC-10	PLC-20	PLC-30

Table 2 Indentation test conditions

Indentation test	
Tip	Steel ball (D: 25.4 mm)
Loading/unloading speed	0.3 mm s^{-1}
Max. load	~1 N

Table 3 Tribo-test conditions

Tribo-test (reciprocating type)	
Tip material (diameter)	Steel ball (D: 1 mm)
Normal load	100/300/500 mN
Sliding speed	4, 16 mm s^{-1}
Sliding stroke	2 mm
Sliding cycle	10 000/100 000/500 000 cycles

main PTFE peak increases. However, no significant changes in the chemical composition are observed with the addition of the lubricant.

The water contact angle and surface roughness of PLCs were measured. The contact angles of all the specimens are shown in Fig. 3(a). The contact angle of the bare PDMS is 99°, and those of PLCs are 103–109°. Water droplets exhibit relatively large contact angles on the hydrophobic PDMS surface owing to its low affinity for water.[36] Because the lubricant added to PDMS is also hydrophobic, PLCs exhibit approximately 4–11% higher contact angles than PDMS.[37] Although no significant differences in the droplet contact angle are observed, the contact angle increases proportionally to the lubricant content. The largest contact angle is observed at the PDMS : lubricant mixing ratio of 100 : 30. As shown in Fig. 3(b), the surface roughness of bare PDMS is 0.36 μm, and those of PLCs are 0.30–1.4 μm. The increase in the surface roughness values of the PLCs compared

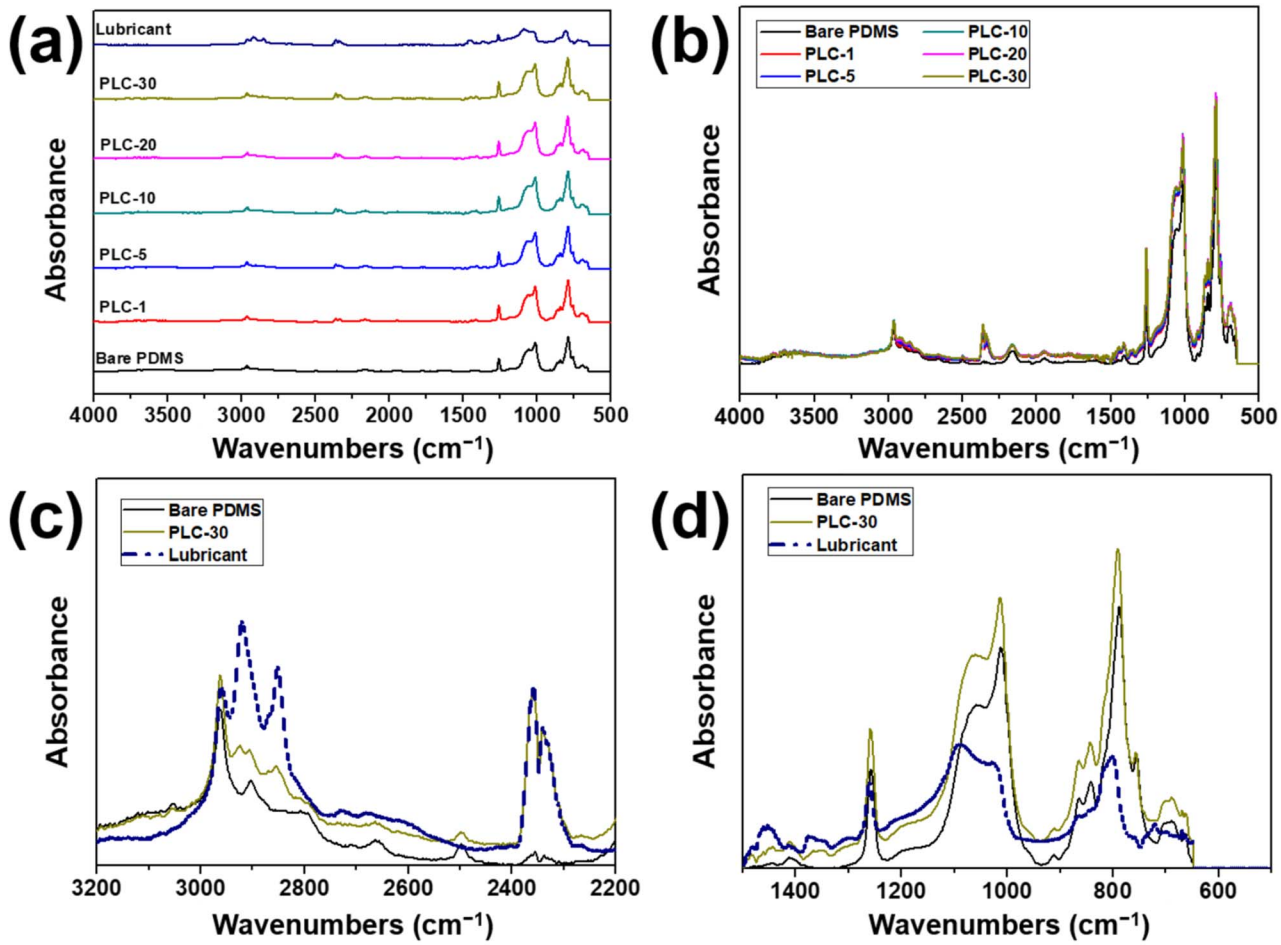

Fig. 2 FTIR spectra of bare PDMS and PLCs according to the mixing ratio of PDMS : lubricant.

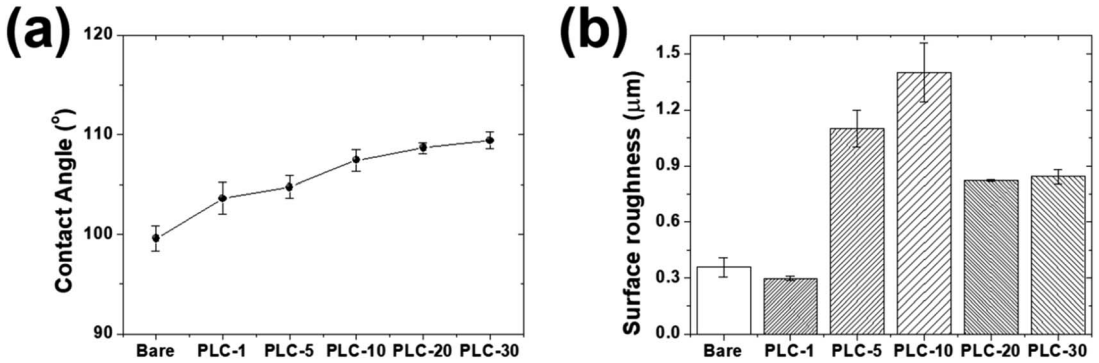

Fig. 3 (a) Contact angle and (b) surface roughness of bare PDMS and PLCs with different PDMS : lubricant mixing ratios.

to bare PDMS were attributed to the effect of the lubricant and the change in the surface conditions during curing.

The relationship between the load and indentation depth was derived using the data obtained in the indentation test, and the elastic modulus was calculated using eqn (1)–(4).[38]

$$h_c = h_m - \frac{3}{4}\frac{F_m}{\left(\frac{dF}{dh}\right)} \quad (1)$$

$$A = \pi(2Rh_c - h_c^2) \quad (2)$$

$$E_r = \frac{1}{2}\left(\frac{dF}{dh}\right)\sqrt{\frac{\pi}{A}} \quad (3)$$

$$\frac{1}{E_r} = \frac{(1-\nu_1^2)}{E_1} + \frac{(1-\nu_2^2)}{E_2} \quad (4)$$

Here, h_c is the contact depth, dF/dh is the stiffness, F_m is the maximum load, R is the radius of the indenter, A is the actual contact area, E_1 is the elastic modulus of the specimen, ν_1 is the Poisson's ratio of the specimen, E_2 is the elastic modulus of the indenter, and ν_2 is the Poisson's ratio of the indenter. The elastic moduli of the specimens are listed in Table 4. The elastic modulus was calculated to be 1.02 MPa for bare PDMS and 1.01–0.77 MPa for PLCs. Thus, the elastic modulus of PDMS is reduced by the addition of lubricants. This result was anticipated because the added lubricant interferes with the bonding between molecules during PDMS curing.

The frictional properties of the specimens were evaluated by performing 10 000 reciprocating sliding movements at sliding speeds of 4 and 16 mm s^{-1} under a normal load of 100 mN. As listed in Table 4, the contact pressure is 0.52 MPa for bare PDMS and 0.43–0.52 MPa for PLCs.[39] The PLCs showed lower contact pressure than bare PDMS because of the decrease in elastic modulus with increasing lubricant content. Fig. 4(a) shows the friction coefficients for all the specimens at sliding speeds of 4 and 16 mm s^{-1}. At a sliding speed of 4 mm s^{-1}, the average friction coefficient of the bare PDMS is 1.00, and that of PLC-1 is 0.94. PLC-1 shows a slightly weaker surface adhesion compared with bare PDMS, but surface adhesion is still observed for this specimen. Because the contact area between PLC-1 and the counter tip increased owing to the decreased mechanical properties of PLC-1, the resistance to sliding of the counter tip is thought to have slightly increased.[9,40] In PLC-5 (ratio of 100 : 5), the friction coefficient (0.16) is significantly lower than in bare PDMS. As the amount of lubricant increased by approximately five times, the friction coefficient decreased by 5–6 times. PLC-10 (ratio of 100 : 10) shows an even lower friction coefficient (0.06). This value is the lowest among all specimens: it is approximately 63% lower than that of PLC-5 (which has twice lower lubricant content) and 94% lower than that of bare PDMS. PLC-20 and PLC-30 showed friction coefficients of 0.19 and 0.28, respectively. That is, with increasing lubricant content, the friction coefficient first decreases but increases after the 100 : 10 ratio. The optimum self-lubricating effect is observed in PLC-10 (PDMS/lubricant ratio of 100 : 10). Overall, all PLCs show lower friction coefficients than bare PDMS. As shown in the previous studies, bare PDMS exhibits a high friction coefficient, and the friction properties of PLCs proposed in this study are better than those of PDMS owing to the self-lubricating properties of the surface.[12,41]

The friction coefficients of the bare PDMS and PLC-1 at the sliding speed of 16 mm s^{-1} are 1.05 and 1.02, respectively, which is a 5–9% increase over the values observed at 4 mm s^{-1}. At a faster sliding speed, the resistance to sliding of the counter tip is expected to be higher because the pressed traces and stresses formed on the specimen surface by the tip are larger and recover to a lower extent.[42,43] In the cases of PLC-5 and PLC-10, although the friction coefficient slightly increases with the increase in sliding speed, the values are very similar. In the cases of PLC-20 and PLC-30, although the friction coefficients slightly decreased with the increase in sliding speed, the values were still very similar. That is, in bare PDMS, PLC-1, PLC-5, and PLC-10, the friction coefficients at a sliding speed of 16 mm s^{-1}

Table 4 Elastic modulus and contact pressure of bare PDMS and PLCs with different PDMS : lubricant ratios

Specimens	Elastic modulus (MPa)	Contact pressure (MPa)
Bare PDMS	1.02	0.52
PLC-1	1.01	0.52
PLC-5	1.00	0.52
PLC-10	0.81	0.45
PLC-20	0.84	0.46
PLC-30	0.77	0.43

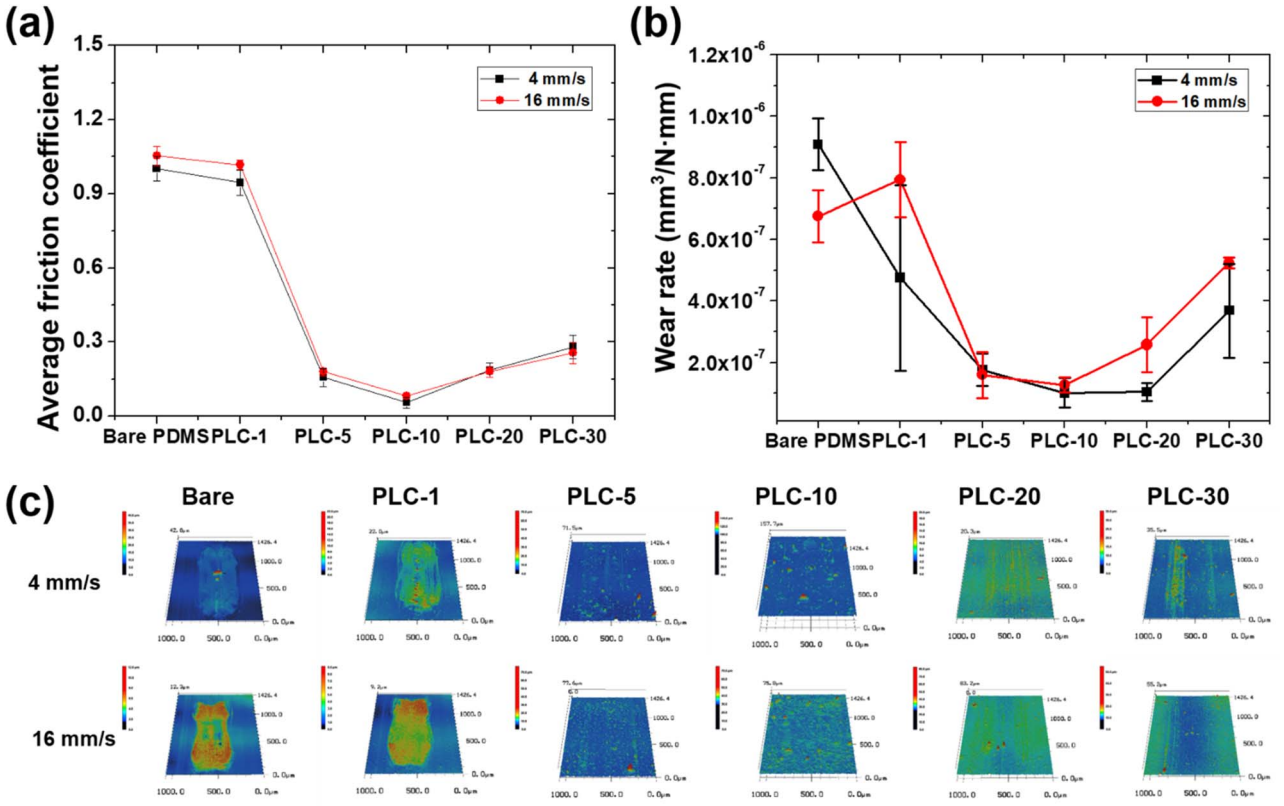

Fig. 4 Friction and wear characteristics of bare PDMS and PLCs at two sliding speeds: (a) average friction coefficient, (b) wear rate, and (c) 3D LSCM images of wear tracks.

are slightly higher than those at 4 mm s^{-1}; however, in PLC-20 and PLC-30, a reverse trend is the case. However, the friction coefficients for each specimen do not significantly differ at different sliding speeds. At the same time, the trend in the friction coefficient with increasing lubricant content is the same regardless of the sliding speed. In PLC-5 and specimens with higher lubricant content, a lubricant film is formed on the surface, and despite the lower mechanical properties than bare PDMS, the friction coefficient is reduced owing to contact between the counter tip and the lubricant film, and the effect of the sliding speed is small.[40,44] Therefore, in bare PDMS and PLC-1, the friction coefficient is high owing to the adhesive properties of the surface. However, with increasing lubricant content, a lubricating film forms on the surface, decreasing the friction coefficient. Overall, the effect of the surface lubricating film on the friction properties seems to be greater than that of the mechanical properties.

Fig. 4(b) shows the wear rates of specimens at two sliding speeds. The wear tracks formed on the surfaces of the specimens were observed using a 3D LSCM to determine the wear volume. The volume of the worn part was measured by analyzing the three-dimensional morphology of the wear tracks formed on the surface of each specimen. The wear rate was obtained by dividing the wear volume by the normal load and total sliding distance. At a sliding speed of 4 mm s^{-1}, the wear rates of bare PDMS, PLC-1, PLC-5, PLC-10, PLC-20, and PLC-30 are 9.09×10^{-7}, 4.75×10^{-7}, 1.76×10^{-7}, 1.00×10^{-7}, 1.04×10^{-7}, and 3.68×10^{-7} $mm^3\ N^{-1}\ mm^{-1}$, respectively. The wear rate is the highest for bare PDMS and initially decreases with increasing lubricant content. The lowest wear rate is observed for PLC-10, and with further increase in the lubricant content, the wear rate increases. The trend in the wear rate with increasing lubricant content changes similar to the trend in the friction coefficient. At the sliding speed of 16 mm s^{-1}, the wear rates of bare PDMS, PLC-1, PLC-5, PLC-10, PLC-20, and PLC-30 are 6.75×10^{-7}, 7.94×10^{-7}, 1.6×10^{-7}, 1.27×10^{-7}, 2.58×10^{-7}, and 5.24×10^{-7} $mm^3\ N^{-1}\ mm^{-1}$, respectively. At a sliding speed of 16 mm s^{-1}, the trend in the wear rate with increasing lubricant content is basically the same as that at a sliding speed of 4 mm s^{-1}, except for bare PDMS. At a sliding speed of 16 mm s^{-1}, PLC-10 also exhibits the lowest wear rate. As shown in Fig. 4(c), severe wear tracks were formed on the surfaces of bare PDMS and PLC-1, whose wear rates are high. Because of the small lubricant content, PLC-1 exhibits no significant changes in the elastic modulus and adhesive properties compared to PDMS; therefore, wear mechanism, in this case, is considered to be similar to that in bare PDMS. In PLC-10, which shows the lowest wear rate, the wear track is not clearly visible, and only slight wear traces are observed. Thus, the size and depth of the wear track on the surface of the specimen correspond to the wear rate. Although the wear rate of PLC-5 is slightly higher than that of PLC-10, the values are almost the same. The wear track of

PLC-5 is slightly more defined compared to that of PLC-10, but the wear patterns are very similar. Thus, the friction coefficient and wear volume decrease with increasing lubricant content until PLC-10 (PDMS/lubricant = 100 : 10), in which slight wear tracks are also observed.[11,12] As the surface of PLCs wears out, the lubricant contained therein comes out and lubricates the contact surfaces, which is thought to improve the friction and wear characteristics. However, in PLC-20 and PLC-30, which have higher lubricant contents than PLC-10, the friction coefficient and wear rate increase with the lubricant content, and the morphology of the wear track is more severe. Thus, when the lubricant content exceeds a certain value, the mechanical properties of PDMS are considerably reduced, and friction increases because of the resistance caused by lubricant viscosity, which leads to stronger wear.[12,41] Higher lubricant content increases the lubrication efficiency, but also causes incomplete curing by blocking the formation of bonds between PDMS molecules during the curing. Thus, specimens with high lubricant contents could not withstand the stress generated in the incompletely hardened specimen during repeated sliding motion. That is, in the cases of PLC-20 and PLC-30, the surface durability of PDMS decreased because the lubricant content is higher than the optimal value, resulting in scratches, and the friction coefficient increased because of the roughened surface. Therefore, an appropriate amount of lubricant is an important condition for optimizing the friction and wear characteristics of PLCs.

In the case of bare PDMS, the morphology of the wear track slightly differs depending on the sliding speed. When a load is repeatedly applied to the surface of the PDMS under low-speed sliding conditions (4 mm s^{-1}) for a long time, compressed PDMS partially recovers between the adjacent cycles. The surface of PDMS shows abrasive wear because it is scratched by the tip as the compression and recovery are repeated during sliding contact.[41] However, under high-speed sliding (16 mm s^{-1}), the compressed PDMS does not manage to recover between the cycles; therefore, PDMS in the compressed state is loaded by the tip that slides again, leading to the accumulation of fatigue because of the residual stress under the surface of the PDMS. It is thought that cracks occurred in this part, and the damaged part was torn in a lump. It is believed that the wear particles torn off by repeated sliding motion were crushed on the PDMS surface.[41] In addition, the wear intensified because during fast sliding motion the specimen and the counter tip do not dissipate the frictional heat and cool down between their contact in adjacent cycles, as opposed to slow sliding motion. As a result, materials such as PDMS and rubber, which are viscoelastic in nature, repeat the compression-recovery process while friction occurs in contact with the mating surface. Therefore, the friction/wear characteristics of these materials tend to differ from those of general metals. This phenomenon can be explained by the Schallamach wave, in which the surface of a viscoelastic material shows a wave perpendicular to the sliding direction when a viscoelastic material makes a relative motion in contact.[45,46] In other words, the interface is not uniform, and movement is possible through local wave propagation across the entire length of the contact interface. A common characteristic of the Schallamach wave is that the separated regions of the contact propagate through the interface to form a wave, resulting in stick–slip and rough wear patterns on the surface. Therefore, in the bare PDMS, there is a difference in the degree and morphology of wear depending on the sliding speed. At the same time, the PLCs show no significant differences in the morphology of the wear track with the change in the sliding speed. In bare PDMS, the degree and pattern of wear differ depending on the sliding speed because the residual stress generated inside the PDMS and the degree of dissipation of frictional heat generated on the surface depend on the sliding speed. However, with the addition of a large amount of lubricant, the effect of sliding speed disappeared because the residual stress and frictional heat were easily dissipated owing to the mechanical properties of the specimen and lubricant. Among the specimens investigated in this study, PLC-10 (PDMS/lubricant = 100 : 10) exhibited the best self-lubricating effect, resulting in improved durability of the PDMS surface.

Fig. 5 shows the friction coefficient, wear volume, wear rate, and wear track morphology of PLC-10, which has the lowest friction coefficient and wear rate, at normal loads of 100, 300, and 500 mN and 10 000, 100 000, and 500 000 sliding cycles. The entire experiment was conducted at a sliding speed of 16 mm s^{-1}. First, in the experiment conducted for 10 000 cycles, the friction coefficient, which is 0.082 at a load of 100 mN, slightly decreases to 0.077 at a load of 300 mN and then significantly increases to 0.130 at a load of 500 mN. At the normal loads of 100, 300, and 500 mN, the wear volume is 508, 1039, and 1135 μm^3, respectively. A threefold increase in the normal load (from 100 to 300 mN) led to an increase in the contact pressure applied to PLC-10, and a slight increase in wear volume; however, no serious scratches are observed on the surface at both normal loads. At the same time, at the normal load of 500 mN, the friction coefficient is nearly twice higher than at 300 mN, because the contact pressure at 500 mN was sufficiently high to cause severe scratch wear on the surface. For 100 000 cycles, the friction coefficients of 0.077, 0.072, and 0.152 under normal loads of 100, 300, and 500 mN, respectively, were obtained, showing similar values to those for 10 000 cycles, whereas the wear volumes slightly increased. At 500 000 cycles, the friction coefficient is 0.05 at the normal load of 100 mN, which is lower than those for 10 000 and 100 000 cycles. At the same time, the friction coefficients at the normal loads of 300 and 500 mN are 0.16 and 0.31, respectively, which are more than twice higher than the corresponding values for 10 000 and 100 000 cycles. For 500 000 cycles, the wear volumes under normal loads of 100 and 300 mN comprised 1370 and 1489 μm^3, respectively, whereas at 500 mN, the wear volume is 7437 μm^3, and serious wear is observed on the surface of PLC-10. Overall, the wear volume and degree of wear track formation are proportional to the normal load and sliding cycles. That is, the increases in the number of sliding cycles and vertical load both lead to more severe wear. However, the wear rate ($mm^3\ N^{-1}\ mm^{-1}$), which is obtained by dividing the wear volume by the normal load and sliding distance, shows the opposite trends with respect to the normal load and sliding cycles. Under all

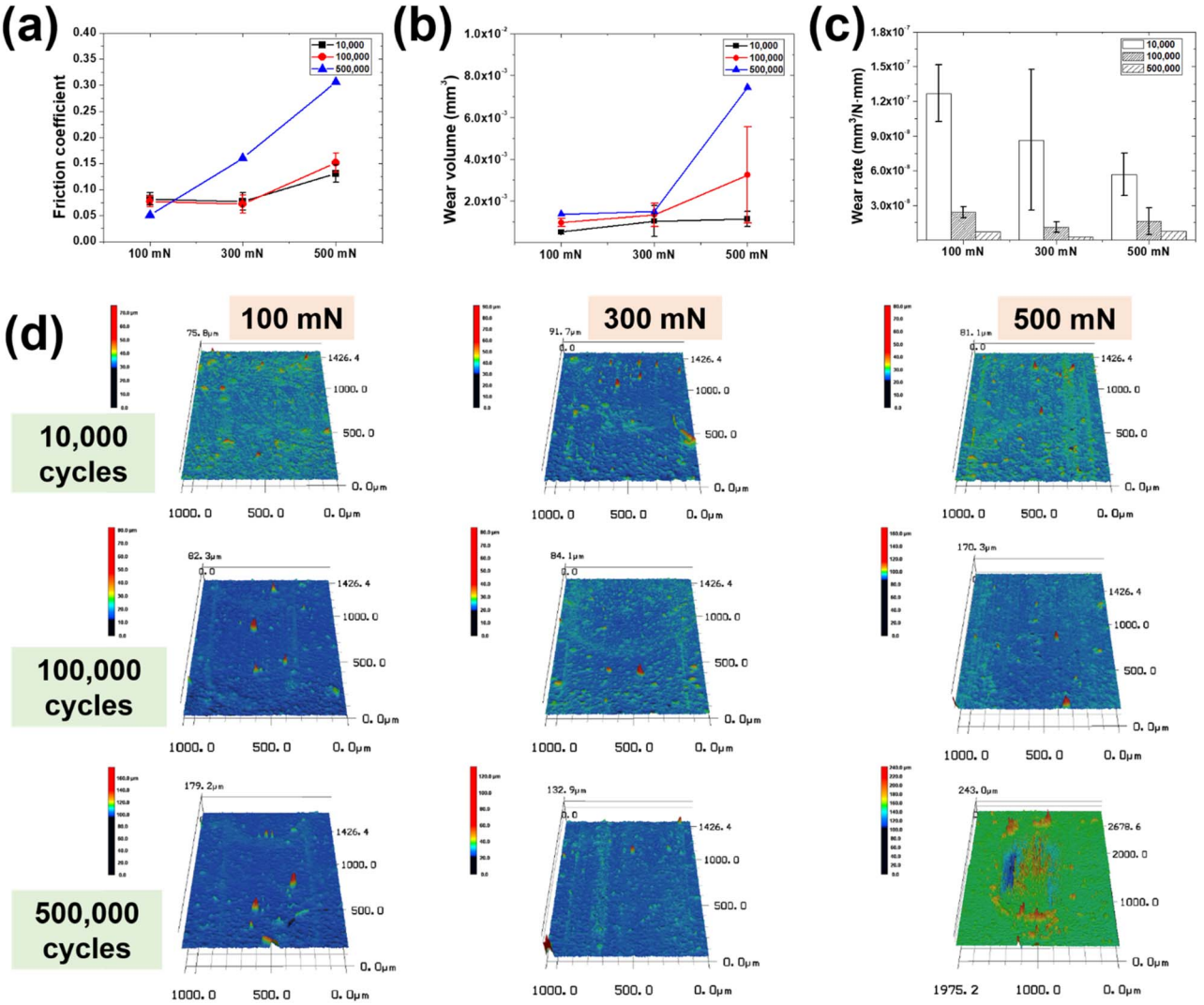

Fig. 5 Friction and wear characteristics of PLC-10 at different normal loads: (a) average friction coefficient, (b) wear volume, (c) wear rate, and (d) 3D LSCM images of wear tracks.

vertical loads (100, 300, and 500 mN), the wear rates at 10 000 cycles are high; at the same time, they tend to significantly decrease at 100 000 and 500 000 cycles. In other words, under the same vertical load, the wear rate decreased with increasing number of sliding cycles. Although the degree of wear increased with the number of sliding cycles, the rate at which wear occurred decreased after a certain number of sliding cycles. Under the same vertical load, because the wear volume increases at a lower rate than the number of sliding cycles, the wear rate (wear volume divided by the vertical load and sliding distance) decreased. Damage to the surface of the PLC-10 specimen led to the release of the lubricant present inside the specimen and self-lubrication, thereby causing the wear rate to decrease with the increase in the number of sliding cycles. In the first 10 000 cycles, the wear rate decreases with increasing normal load, whereas for 100 000 and 500 000 cycles, the wear rate is the lowest under a vertical load of 300 mN. This implies that in the first 10 000 cycles, the wear rate is lower than the rate at which the normal load was increased. In other words, an increase in the normal load did not significantly accelerate wear. In the case of the increased sliding motion for 100 000 cycles, the occurrence of wear did not worsen as much as the increase in the normal load in the case of 300 mN compared to the case of 100 mN, but the acceleration of wear in the case of 500 mN was higher than that in the case of 300 mN. For 500 000 cycles, the wear rate is the highest at the normal load of 500 mN and the lowest at 300 mN. Overall, the wear rate is the lowest for 500 000 cycles under a normal load of 300 mN. As shown in Fig. 5(d), at a normal load of 500 mN, severe wear tracks were formed, whereas at a normal load of 300 mN, the wear tracks are considerably less pronounced. In this study, the PLC-10 specimen exhibited the best friction and wear characteristics because its self-lubrication was maintained for at least 500 000 cycles at normal loads of 300 mN or less.

Fig. 6 shows the results of the finite element analysis (FEA) using ABAQUS performed to compare the internal stress

behaviors during indentation and contact sliding at different speeds for bare PDMS and PLC-10. The tested bare PDMS and PLC-10 specimens had a size of 4 mm × 2 mm and thickness of 1 mm. The elastic modulus obtained in the indentation test and the friction coefficients obtained in the friction test were used as the mechanical and friction properties of the specimens in the simulation; a steel ball with a diameter of 1 mm, the same as that in the friction test, was chosen as the counter tip. The elastic modulus and Poisson's ratio of the steel ball were 210 GPa and 0.3, respectively.[47] The simulation analysis conditions were set as follows: to the fixed specimens, a load of 100 mN was applied with a counter tip, followed by sliding a stroke of 2 mm. As shown in Fig. 7, both the contact pressure and von Mises stress of the bare PDMS are higher than those of the PLC-10. In both specimens, stress was generated on the surface contacting with the counter material and propagated around the contact point. This is a characteristic of elastic PDMS, and the stress is expected to be dispersed by the elastic stiffness of the PDMS specimen.[48–51] In addition, the stress of the contact part tends to be proportional to the mechanical properties of the specimen. Next, the sliding motion at speeds of 4 and 16 mm s^{-1} (similar to the actual friction experiment) was analyzed. As shown in Fig. 6 and 7, the stresses generated inside the modeling specimens during the sliding motion at 4 and 16 mm s^{-1} do not significantly differ. However, there is a slight difference in stress between the bare PDMS and PLC-10 models at the same sliding speed, and the stress generated in the bare PDMS at both sliding speeds is greater than that in PLC-10. For each specimen and sliding speed, after the sliding motion progresses to a certain point, the magnitude of the stress generated in the specimen is 5–10% larger than that at the beginning of sliding. As shown in Fig. 6, the stress generated in the specimen during the initial contact and sliding motion is widely distributed under the contact point, even before the counter tip passed. In the initial contact, a widely distributed stress was generated by the normal load and sliding friction of the counter tip; thus, the stress had already been generated at the point inside the specimen in the sliding direction where the counter tip has not yet passed. In this state, when the counter tip passes this point, larger stress is generated because the newly formed stress distribution overlaps with the stress caused by the previous contact. Considering the surface deformation caused by the contact of the elastic PDMS, the surface of the PDMS was press-fitted by the counter tip, and the surface was slightly elevated in the direction of tip sliding. Because of the change in the surface morphological structure, the frictional force caused by blocking increases; the stress also increases because of the structural compression as the counter tip passes over the raised part.

Fig. 8 shows a schematic of the wear mechanism and self-lubrication mechanism during the sliding motion for bare PDMS and PLC-10. The surface of the bare PDMS is press-fitted by the normal load of the counter tip, and the surface rises over the circumference of the tip; this phenomenon is commonly observed in elastic materials. This increases the contact area, and when the sliding motion proceeds, the adhesion also

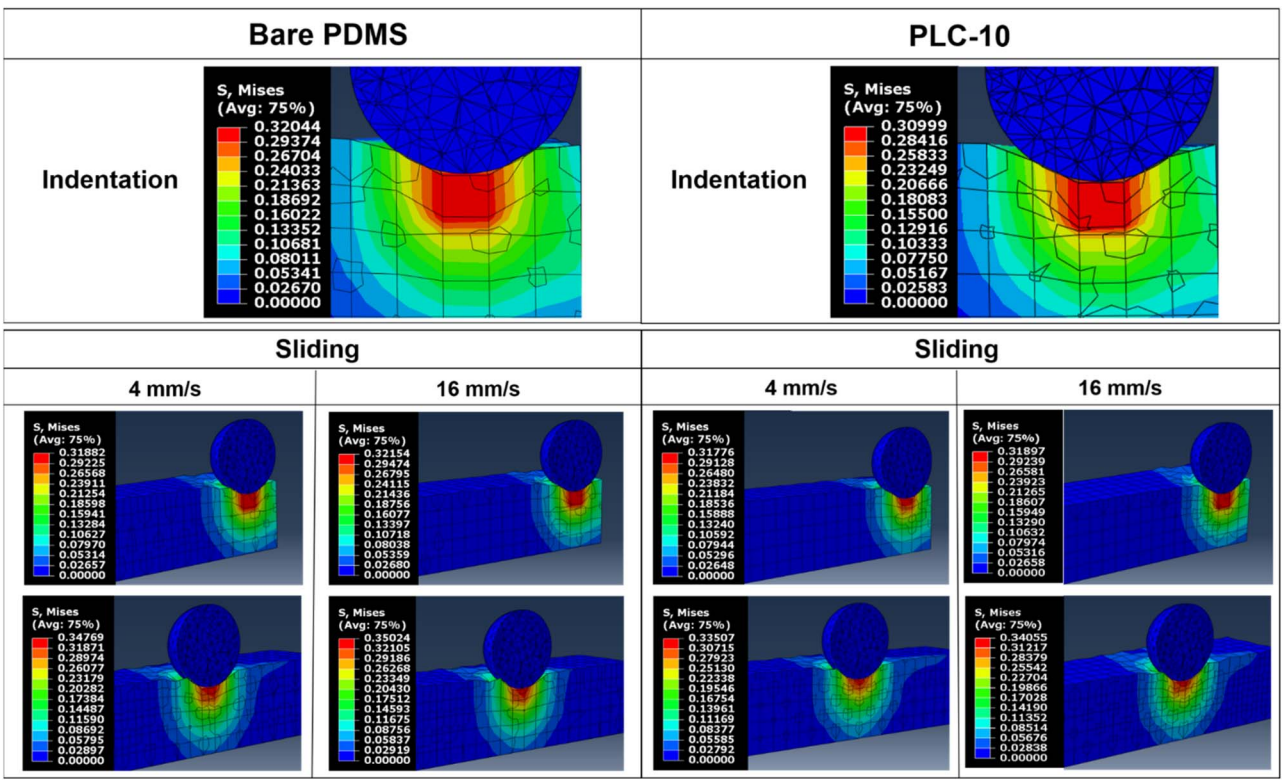

Fig. 6 FEA simulation results for bare PDMS and PLCS-10 at different indentation and sliding speeds.

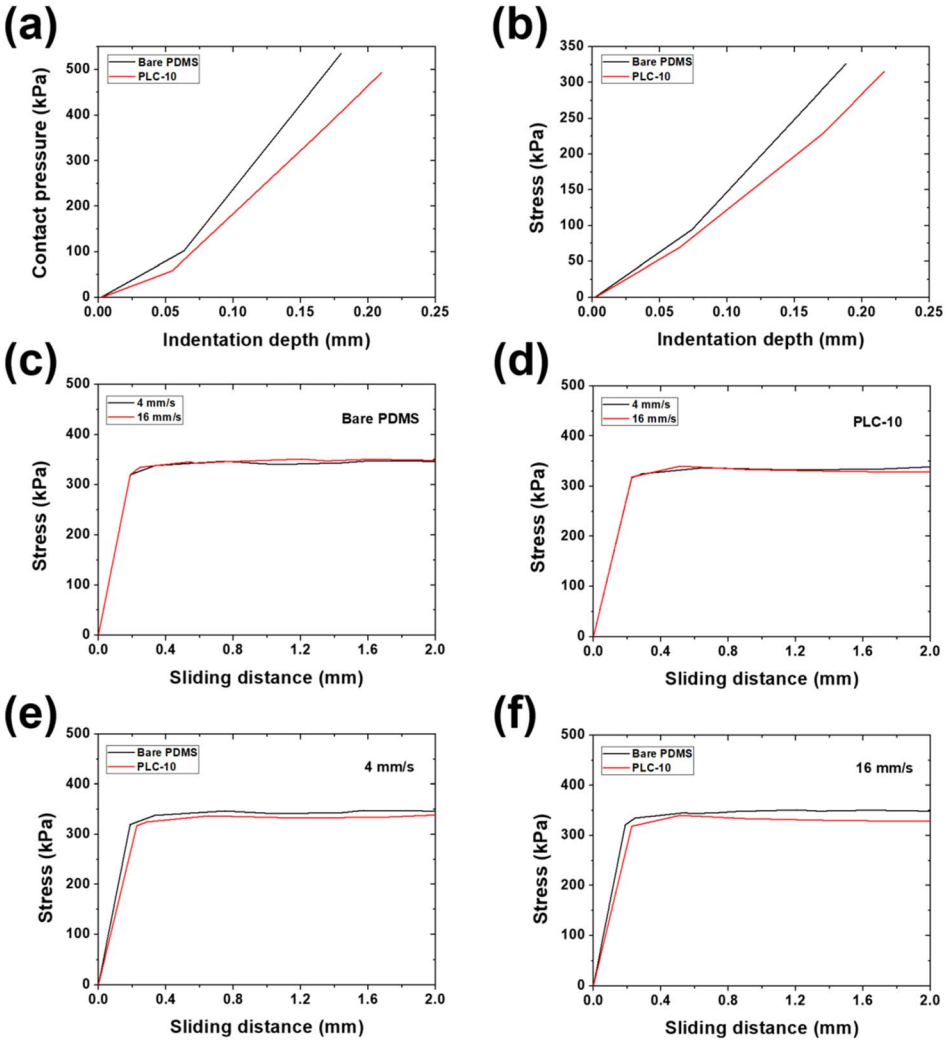

Fig. 7 Results of stress behavior analysis: (a) contact pressure, (b) indentation stress, and (c)–(f) sliding stress of bare PDMS and PLC-10 at different sliding speeds.

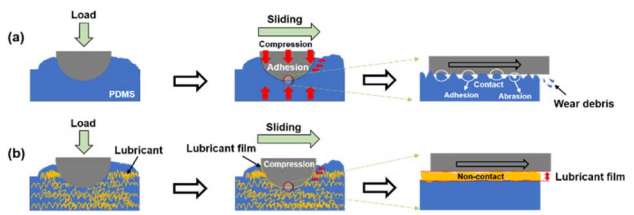

Fig. 8 Schematic designs of wear mechanism of bare PDMS and PLCs.

increases, and the surface of the specimen rises toward the front of the counter tip. The frictional resistance increases because a reaction force that prevents the tip from sliding is generated. For this reason, the friction coefficient of bare PDMS is high ($\geq$1). As the sliding motion is repeated, the adhesion and surface deformation between the counter tip and PDMS surface owing to compression occur again, causing the peel-off of PDMS wear debris. In addition, abrasive wear occurs, in which the relatively soft PDMS surface is ripped off by rough micro-protrusions on the counter tip surface. Thus, adhesive and abrasive wear mechanisms occur simultaneously, forming wear debris, and the surface subjected to the contact sliding motion becomes very rough. Fig. 4(c) also confirms that a rough wear track surface was formed on bare PDMS. In contrast, the surface of PLC-10 rose over the periphery of the counter tip, as in bare PDMS at the initial stage of contact; furthermore, it rose more than in bare PDMS owing to weaker mechanical properties compared to bare PDMS. Because PLC is softer than bare PDMS, the reaction force generated when the tip slid over the raised PLC surface is lower. The friction coefficient of the PLC self-lubricated by the lubricant mixed in the PDMS is 0.06, which is significantly lower than that of bare PDMS. In particular, it is suggested that a lubricant film is formed on the contact interface between the counter tip and PLC-10, such that the two surfaces do not directly contact each other to some extent. Therefore, friction and wear occur differently in bare PDMS and PLC-10 owing to the different contact conditions with the counter tip.

4 Conclusions

In this study, the surface, chemical, mechanical, and tribological properties of PLCs were evaluated. The contact angles of the PLC specimens were higher than that of bare PDMS and increased with the lubricant content. Moreover, the surface roughness increased owing to the effect of the particles present in the lubricant and formed lubricating film. The elastic modulus generally decreased as the amount of lubricant increased. The contact sliding behaviors of bare PDMS and PLC-10 were analyzed through FEA simulation, and the results of the analysis confirmed that the stresses generated in the two specimens are slightly different, but both are weakly affected by the sliding speed. Although the mechanical properties of PLC-10 were worse than those of bare PDMS because of the lubricant addition, the effect on contact conditions was not significant. At the same time, PLCs showed significantly lower friction coefficients than bare PDMS, with PLC-10 exhibiting 94% lower friction coefficient than bare PDMS, which is the lowest value recorded in this study. In PLCs, a lubricating film was formed on the surface owing to excellent self-lubricating properties; thus, the frictional resistance was reduced and almost no wear occurred. The durability of PLC-10 was maintained even after 500 000 cycles of reciprocating sliding under low normal loads (100–300 mN), but relatively severe wear occurred under a high normal load (500 mN). Therefore, it was confirmed that the mixing of the lubricant inside PDMS improves its friction properties, changes the wear mechanism, and increases durability. The results of this study are expected to be helpful in the application of PDMS in electronics and biomedical field, which require lubrication properties and durability.

Author contributions

Sung-Jun Lee: conceptualization, methodology, software, validation, formal analysis, investigation, data curation, writing – original draft, writing – review & editing, visualization. Gang-Min Kim: software, validation, investigation. Chang-Lae Kim: conceptualization, methodology, resources, writing – review & editing, supervision, project administration.

Conflicts of interest

There are no conflicts to declare.

Acknowledgements

This research was supported by Basic Science Research Program through the National Research Foundation of Korea(NRF) funded by the Ministry of Education (2021R1I1A3059770).

References

1 L. Xue, J. T. Pham, J. Iturri and A. Del Campo, *Langmuir*, 2016, **32**, 2428–2435.
2 F. Schneider, J. Draheim, R. Kamberger and U. Wallrabe, *Sens. Actuators, A*, 2009, **151**, 95–99.
3 N. S. Tambe and B. Bhushan, *Ultramicroscopy*, 2005, **105**, 238–247.
4 K. Khanafer, A. Duprey, M. Schlicht and R. Berguer, *Biomed. Microdevices*, 2009, **11**, 503–508.
5 A. Sharfeddin, A. A. Volinsky, G. Mohan and N. D. Gallant, *J. Appl. Polym. Sci.*, 2015, **132**, 42680.
6 R. Seghir and S. Arscott, *Sens. Actuators, A*, 2015, **230**, 33–39.
7 K. L. Johnson, K. Kendall and a. Roberts, *Proc. R. Soc. London, Ser. A*, 1971, **324**, 301–313.
8 M. Barquins, *Wear*, 1993, **160**, 1–11.
9 C. Charitidis, *Int. Scholarly Res. Not.*, 2011, **2011**, 719512.
10 J. Greenwood, H. Minshall and D. Tabor, *Proc. R. Soc. London, Ser. A*, 1961, **259**, 480–507.
11 J. Bongaerts, K. Fourtouni and J. Stokes, *Tribol. Int.*, 2007, **40**, 1531–1542.
12 T.-L. Park, Y.-M. Yang, D.-G. Shin and D.-E. Kim, *J. Korean Soc. Precis. Eng.*, 2018, **35**, 803–807.
13 C. Dong, L. Shi, L. Li, X. Bai, C. Yuan and Y. Tian, *Tribol. Int.*, 2017, **106**, 55–61.
14 B.-B. Jia, T.-S. Li, X.-J. Liu and P.-H. Cong, *Wear*, 2007, **262**, 1353–1359.
15 T. Luo, X. Wei, X. Huang, L. Huang and F. Yang, *Ceram. Int.*, 2014, **40**, 7143–7149.
16 C.-Y. Chen, C.-L. Chang, T.-F. Chien and C.-H. Luo, *Sens. Actuators, A*, 2013, **203**, 20–28.
17 C. Hassler, T. Boretius and T. Stieglitz, *J. Polym. Sci., Part B: Polym. Phys.*, 2011, **49**, 18–33.
18 B. Liu, Y. Chen, Z. Luo, W. Zhang, Q. Tu and X. Jin, *J. Biomater. Sci., Polym. Ed.*, 2015, **26**, 1229–1235.
19 J. H. Lee, Y. W. Nam, H.-C. Jung, D.-H. Baek, S.-H. Lee and J. S. Hong, *BioChip J.*, 2012, **6**, 91–98.
20 B. He, W. Chen and Q. J. Wang, *Tribol. Lett.*, 2008, **31**, 187–197.
21 W. Huang, L. Jiang, C. Zhou and X. Wang, *Tribol. Int.*, 2012, **52**, 87–93.
22 B.-H. Ryu and D.-E. Kim, *CIRP Ann. Manuf. Technol.*, 2015, **64**, 519–522.
23 E. Ahmed, A. Nabhan, N. M. Ghazaly and G. Abd El Jaber, *Am. J. Nanomater.*, 2020, **8**, 1–9.
24 P. M. Lugt, *Tribol. Trans.*, 2009, **52**, 470–480.
25 X.-D. Yuan and X.-J. Yang, *Wear*, 2010, **269**, 291–297.
26 S. Biswas and K. Vijayan, *Wear*, 1992, **158**, 193–211.
27 H. Lu, W. Tang, X. Liu, B. Wang and Z. Huang, *J. Mater. Sci.*, 2017, **52**, 4483–4492.
28 E. Dhanumalayan and G. M. Joshi, *Adv. Compos. Hybrid Mater.*, 2018, **1**, 247–268.
29 F. X. Borras, M. B. De Rooij and D. J. Schipper, *Lubricants*, 2018, **6**, 100.
30 D. Sun, B.-B. Li and Z.-L. Xu, *Korean J. Chem. Eng.*, 2013, **30**, 2059–2067.
31 J. Coates, *Encyclopedia of analytical chemistry: applications, theory and instrumentation*, 2006.
32 K. Yamauchi, Y. Yao, T. Ochiai, M. Sakai, Y. Kubota and G. Yamauchi, *J. Nanotechnol.*, 2011, **2011**, 380979.
33 J. Lee, J. Kim, H. Kim, Y. M. Bae, K.-H. Lee and H. J. Cho, *J. Micromech. Microeng.*, 2013, **23**, 035007.

34 J. J. Shao, W. Tang, T. Jiang, X. Y. Chen, L. Xu, B. D. Chen, T. Zhou, C. R. Deng and Z. L. Wang, *Nanoscale*, 2017, **9**, 9668–9675.
35 Y. Kimura, N. Mizusawa, A. Ishii, T. Yamanari and T.-a. Ono, *Biochemistry*, 2003, **42**, 13170–13177.
36 H. T. Kim and O. C. Jeong, *Microelectron. Eng.*, 2011, **88**, 2281–2285.
37 S.-M. Lee, S. H. Kim, J. H. Lee, S.-J. Lee and H.-K. Kim, *RSC Adv.*, 2018, **8**, 18508–18518.
38 N. Oumarou, J.-P. Jehl, R. Kouitat and P. Stempfle, *Int. J. Surf. Sci. Eng.*, 2010, **4**, 416–428.
39 A. Fischer-Cripps, *J. Mater. Sci.*, 1999, **34**, 129–137.
40 R. Chou, A. H. Battez, J. Cabello, J. Viesca, A. Osorio and A. Sagastume, *Tribol. Int.*, 2010, **43**, 2327–2332.
41 C. L. Johnson and A. C. Dunn, *Wear*, 2019, **438**, 203066.
42 D. Moore and W. Geyer, *Wear*, 1972, **22**, 113–141.
43 V. Zankin and W. Yandell, *Wear*, 1981, **72**, 157–185.
44 T. Zolper, Z. Li, C. Chen, M. Jungk, T. Marks, Y.-W. Chung and Q. Wang, *Tribol. Lett.*, 2012, **48**, 355–365.
45 A. Schallamach, *Wear*, 1971, **17**, 301–312.
46 S. Maegawa and K. Nakano, *Wear*, 2010, **268**, 924–930.
47 S.-J. Lee, G.-M. Kim and C.-L. Kim, *Coatings*, 2021, **11**, 603.
48 C.-L. Kim and D.-E. Kim, *Sci. Rep.*, 2017, **7**, 1–11.
49 D.-E. Kim, C.-L. Kim and H.-J. Kim, *CIRP Ann. Manuf. Technol.*, 2011, **60**, 599–602.
50 C.-L. Kim, C.-W. Jung, Y.-J. Oh and D.-E. Kim, *NPG Asia Mater.*, 2017, **9**, e438.
51 C.-L. Kim and D.-E. Kim, *Sci. Rep.*, 2016, **6**, 1–11.